


An ultrastructural study of chondroptosis: programmed cell death in degenerative intervertebral discs *in vivo*

Li-Bo Jiang, Hai-Xiao Liu, Yu-Long Zhou, Sun-Ren Sheng, Hua-Zi Xu and En-Xing Xue 

Department of Orthopedic Surgery, The Second Affiliated Hospital and Yuying Children's Hospital of Wenzhou Medical University, Wenzhou, Zhejiang, China

Abstract

Apoptosis has been regarded to mediate intervertebral disc degeneration (IDD); however, the basic question of how the apoptotic bodies are cleared in the avascular intervertebral disc without phagocytes, which are essential to apoptosis, remains to be elucidated. Our goals were to investigate the ultrastructure of nucleus pulposus (NP) cells undergoing chondroptosis, a variant of apoptotic cell death, in a rabbit annular needle-puncture model of IDD. Experimental IDD was induced by puncturing discs with a 16-G needle in New Zealand rabbits. At 4 and 12 weeks after puncture, progressive degeneration was demonstrated by X-ray, magnetic resonance imaging and histological staining. TUNEL staining suggested a significant increase in the apoptosis index in the degenerated NP. However, the percentage of apoptotic cells with the classic ultrastructure morphology was much less than that with chondroptotic ultrastructure morphology under transmission electron microscopy (TEM). The chondroptotic cells from the early to late stage were visualized under TEM. In addition, the percentage of chondroptotic cells was significantly enhanced in the degenerated NP. Furthermore, 'paralyzed' cells were found in the herniated tissue. Western blotting revealed an increase in caspase3 expression in the degenerated NP. The expression of the Golgi protein (58K) was increased by the fourth week after puncture but decreased later. These findings indicate that chondroptosis is a major type of programmed cell death in the degenerated rabbit NP that may be related to the progressive development of IDD.

Key words: animal model; apoptosis; chondroptosis; intervertebral disc degeneration.

Introduction

Intervertebral disc degeneration (IDD) is considered a major cause of low-back pain (Miyagi et al. 2014). However, the pathophysiological mechanism is still unclear. Factors that influence the process of disc degeneration include abnormal mechanical loading, unfavorable inheritance, smoking, obesity and aging (Kelempisioti et al. 2011; Vo et al. 2011; Paul et al. 2012; Samartzis et al. 2012). In intervertebral discs (IVDs) these factors increase the risk of cell death, which further reduces synthesis of extracellular matrix components (Zhao et al. 2007).

Apoptosis, the type I programmed cell death, has been reported to be involved in IDD induced by different stimulators such as mechanical and structural stimulation (Sudo &

Minami, 2011; Ding et al. 2012). Furthermore, suppression of apoptosis via siRNA also leads to regeneration of IVDs (Sudo & Minami, 2011). Apoptosis distinct from pathological necrosis is characterized by nuclear condensation, fragmentation and budding into apoptotic bodies within the lipid membranes, followed by shrinkage of the cytoplasmic membrane and rapid phagocytosis of dead cells (Kerr et al. 1972). Although the ultrastructure of classical apoptosis was observed in cell culture (Gruber et al. 2000), it is rarely investigated thoroughly *in vivo*, where TUNEL staining instead of transmission electron microscopy (TEM) is always used. The final apoptotic body is generally cleared from the system via phagocytosis by macrophages, reducing the possibility of subsequent inflammation, which is used to distinguish apoptosis from necrosis. However, there are no phagocytes in nucleus pulposus (NP) tissue due to the lack of blood supply in IVDs (Roberts et al. 2006). In addition, the NP cells embedded within the matrix are isolated from other cells. Therefore, we speculate that there is another form of cell death in addition to classical apoptosis *in vivo* during IDD.

Variations of apoptosis have been reported, including paraptosis and lipoapoptosis (Kakisaka et al. 2012; Wang

Correspondence

En-Xing Xue, Department of Orthopedic Surgery, The Second Affiliated Hospital and Yuying Children's Hospital of Wenzhou Medical University, 109 Xueyuan Western Road, Wenzhou, Zhejiang 325027, China. T: +86 0577 88002808; F: +86 0577 88002808; E: xueenxing@163.com

Accepted for publication 9 March 2017
Article published online 24 April 2017

et al. 2012). Dark cells, which may be a type of programmed cell death in non-classical cases, have also been found in several species (Anderson, 1964; Roach & Clarke, 2000; Roach et al. 2004; Perez et al. 2005; Ahmed et al. 2007; Chen et al. 2010). These studies defined dark chondrocytes as chondroptotic cells, with a characteristic morphology different from that observed in classical apoptosis. Under TEM, typical apoptotic cells exhibit condensed nuclear chromatin, a shrunken cell membrane and blebbing of apoptotic bodies. In contrast, chondroptotic cells are dark and have extensive endoplasmic reticulum (ER) blebbing of cytoplasmic vacuoles, a ruptured cell membrane and vacuole discharge. In alkaptotic cartilage, chondroptosis has also been observed (Millucci et al. 2015). The biochemistry of IVDs is known to resemble that of articular cartilage, and the NP cells transform into chondrocyte-like cells upon IDD. Importantly, chondroptotic cells have also been found in the annulus fibrosus (AF) of degenerated discs collected from patients (Sitte et al. 2009, 2012); however, the existence of chondroptotic cells in the NP remains unclear. In addition, these cells have been found in cervical discs rather than in the lumbar discs that are regarded as the main component of disc herniation in patients, and the morphological description of chondroptotic cells might not be systematic enough. Considering the above findings, we hypothesized that chondroptosis is the major type of programmed cell death in the NP. In the present study, we systematically elucidated the existence and role of chondroptosis in the degenerated NP using a rabbit annular needle-puncture model of IDD.

Materials and methods

All animal experiments were approved by the ethical committee for animal experimentation of WenZhou Medical College, Zhejiang, China.

Rabbit model of IDD

The widely accepted needle-puncture rabbit model of IDD was performed using 30 male 1-year-old New Zealand rabbits in conventional housing, weighing approximately 3–3.5 kg each. Twenty out of the 30 rabbits were randomized into a model group with 10 rabbits in the 4-week group and 10 in the 12-week group. After anesthesia with 10% trichloroacetaldehyde monohydrate administered intraperitoneally (3 mL kg^{-1}), the rabbits were placed in a lateral prone position. A posterolateral retroperitoneal approach was used to expose the anterior surface of three consecutive lumbar IVDs (L3–4 to L5–6), according to the location of L5–6 discs corresponding to the pelvic rim. The L3–4 and L5–6 discs were punctured from the AF into the NP for 5 s using a 16-G needle parallel to the endplates. The depth was controlled at precisely 5 mm as described previously (Masuda et al. 2005), while the L4–5 disc was left intact as an internal control. The remaining 10 rabbits were not punctured and served as the control group. After the operation, three rabbits out of the 10 were killed for histology analysis, and the other rabbits were killed for TEM and Western blotting.

Imaging and histomorphology

Following anesthesia, radiological and magnetic resonance imaging (MRI) investigations were performed at 4 and 12 weeks postoperatively under a strict protocol, as previously described (Masuda et al. 2005). The preoperative images were used as a baseline measure. To confirm the progressive degeneration of punctured IVDs compared with that of the normal discs, the disc height index (DHI) and modified Thompson classification were evaluated by two experts in the image archiving and communication system at our hospital. These normal and punctured discs containing adjacent endplates, and minimal vertebral body were harvested from the rabbits after death. They were fixed in 10% neutral formalin and decalcified with 10% EDTA, followed by paraffin embedding. The 5- μm -thick mid-sagittal sections were stained with hematoxylin and eosin (H & E). These sections were analyzed using a grading scale (Masuda et al. 2005) to semiquantitatively evaluate disc degeneration under a light microscope.

TUNEL assay

Dewaxed IVD sections were incubated with $15 \mu\text{g mL}^{-1}$ of proteinase K for 15 min at 37°C . Following treatment with 3% H_2O_2 to quench the endogenous peroxidase for 5 min at room temperature, the specimens were washed three times with phosphate-buffered saline (PBS) and detected for cell death *in situ* (Roche, Mannheim) according to the manufacturer's instructions. The sections treated with DNase (2 U mL^{-1}) for 1 h and processed without terminal transferase served as the positive and negative controls, respectively. The positive percentage was calculated by selecting similar regions in these sections to determine the number of positive-stained cells under light microscopy (magnification $\times 200$).

TEM

The samples including the NP and the herniated tissue located in the punctured area at the anterolateral part of the discs were dissected into three cubes (approximately $1 \text{ mm} \times 2 \text{ mm}$) and fixed in 2.5% glutaraldehyde overnight. They were washed with PBS three times, post-fixed in 2% osmium tetroxide and block-stained with 2% uranyl acetate. Following dehydration in an acetone series, these cubes were embedded in Araldite. The semi-thin sections were subjected to toluidine blue staining to observe the location of the cells. Finally, ultra-thin sections of at least three blocks derived from a single disc were visualized under a Hitachi TEM (Katsuta, Ibaraki, Japan). In a section of NP tissue, at least 13–15 cells and six fields of view were examined to determine the percentage of chondroptotic cells and cells showing classical apoptosis. Under TEM, condensed nuclear chromatin, shrunken cell membrane and blebbing of apoptotic bodies were used to identify the typical apoptotic cells. Dark cells with extensive ER blebbing of cytoplasmic vacuoles, a ruptured cell membrane and vacuole discharge were used to distinguish the chondroptotic cells. All chondroptotic cells in the early, middle and late stages were included in the calculation. The Bland-Altman method and MedCalc software (MedCalc, Mariakerke, Belgium) were used to evaluate the level of inter-observer and intra-observer agreement in the number of apoptotic and chondroptotic cells.

Western blotting for caspase 3 and 58K Golgi protein

At 4 and 12 weeks after the puncture, the NP tissue was collected, and the protein was isolated using RIPA lysis buffer with 1 mM phenylmethylsulfonyl fluoride (PMSF; Beyotime, China). The total protein concentration was determined using an enhanced BCA protein assay kit (Beyotime). Each sample of 30 µg protein was separated using sodium dodecyl sulfate–polyacrylamide gel electrophoresis, and transferred to a polyvinylidene difluoride (PVDF) membrane (BIO-RAD, USA). The membranes were soaked for 2 h in 5% non-fat milk and incubated overnight with rabbit polyclonal antibodies against caspase 3 (Abcam; 1 : 500), 58K (Abcam; 1 : 200) and GAPDH (Abcam; 1 : 3000). After washing three times, the membranes were incubated with anti-rabbit horseradish peroxidase-conjugated secondary antibodies, and the bands were detected with the ECL plus (Invitrogen, USA) reagent using enhanced chemiluminescence (PerkinElmer, USA). Finally, the intensity of the bands was quantified using the ALPHA-EASE FC 4.0 software.

Statistical analysis

Statistical analyses were performed using the SPSS 15 statistical software program (SPSS, Chicago, IL, USA). Normality was checked using the Kolmogorov–Smirnov test, and the differences between groups were evaluated by ANOVA or Kruskal–Wallis test. LSD analysis or Mann–Whitney *U*-test was used to explore the differences between two groups, as needed. The Bland–Altman method was used to evaluate the consistency of the intra-observer and inter-observer evaluation. Differences were considered statistically significant at an error level of $P < 0.05$.

Results

Model establishment

Failure to precisely control the dose of the anesthetic led to the death of two rabbits in the model group during the MRI examination. The remaining rabbits completed the experiment successfully without obvious surgical complications.

Histological, radiographic and MRI evaluation

To confirm the IDD after puncture, we evaluated the histology, DHI and MRI scores using H & E staining, X-ray and MRI, respectively. The degeneration of the IVDs involved loss of extracellular matrix. The NP cells were transformed into chondrocyte-like cells, accompanied by disorganization and invagination of the annulus with an indistinct border between the AF and NP compared with that observed in the normal discs (Fig. 1A). Compared with the score of the normal discs, the postoperative histological score at 4 and 12 weeks was significantly higher ($P < 0.01$ at each time point; Fig. 1D). The DHI of L3–4 and L5–6 showed a slow and progressive decrease, and the percentage of DHI at each time point after puncture was significantly smaller than the pre-surgical value ($P < 0.01$; Fig. 1B,E).

Furthermore, the size of the osteophytes adjacent to the punctured discs was increased. Analysis of the MRI scans of rabbits using T2-weighted, midsagittal plane images revealed a gradual decrease in the intensity and area of high signals in L3–4 and L5–6, while the non-punctured L4–5 discs showed a relatively constant signal (Fig. 1C). Using the modified Thompson classification, the punctured discs also showed a progressive degeneration ($P < 0.01$; Fig. 1E).

Apoptosis of NP cells

The positive-stained cells were stained green under fluorescence microscopy and brownish red under light microscopy (Fig. 2A). Few apoptotic NP cells were detected in normal discs ($1.6 \pm 0.8\%$). Compared with that in the normal discs, the degenerated NP contained significantly more apoptotic cells (4 weeks: $7.5 \pm 1.9\%$, $P < 0.01$; 12 weeks: $18.7 \pm 3.2\%$, $P < 0.01$; Fig. 2B).

Ultrastructural morphology

Chondroptotic cells

The NP tissue was observed using TEM to identify the type of programmed cell death. We found that chondroptosis rather than apoptosis was the major programmed cell death present. Chondroptosis was characterized by a series of changes from the early to late stage as follows.

Early stage of chondroptosis. The cells in this stage were characterized by a condensed nucleus and extensive ER. The chondroptotic cells, also known as 'dark' cells, contained a darker nucleus and cytoplasm and were smaller in size compared with that in the healthy cells (Fig. 3D), indicating cellular degeneration. However, unlike the crescent-shaped masses (Fig. 3C) or the sharply delineated mass of apoptotic cells, the chondroptotic cells showed an indented nuclear envelope and small patches of condensed chromatin scattered around the nucleus (Fig. 3E,F). The rER membrane increased and expanded to enclose the cytoplasm and organelles, which were digested or secreted into the extracellular space (Fig. 3H). In addition, the cytoplasm contained many Golgi complexes and blebs (Fig. 3G). Half of the cytoplasm showed a ruptured appearance or protruded to the cell exterior (Fig. 3F), with numerous vesicles including autophagic vacuoles derived from the rER.

Mid-stage of chondroptosis. The nucleus and the cell membrane were hyper-condensed and smaller (Fig. 4B), indicating the relationship between cytoplasmic changes and nuclear alterations. As a result, the morphology of these cells became spindly and darker, and the density of the karyoplasm also increased (Fig. 4A,B). The majority of the cytoplasm and organelles including the Golgi complex disappeared, while the large rER membranes almost filled the cell, restricting the remaining cytoplasm to a

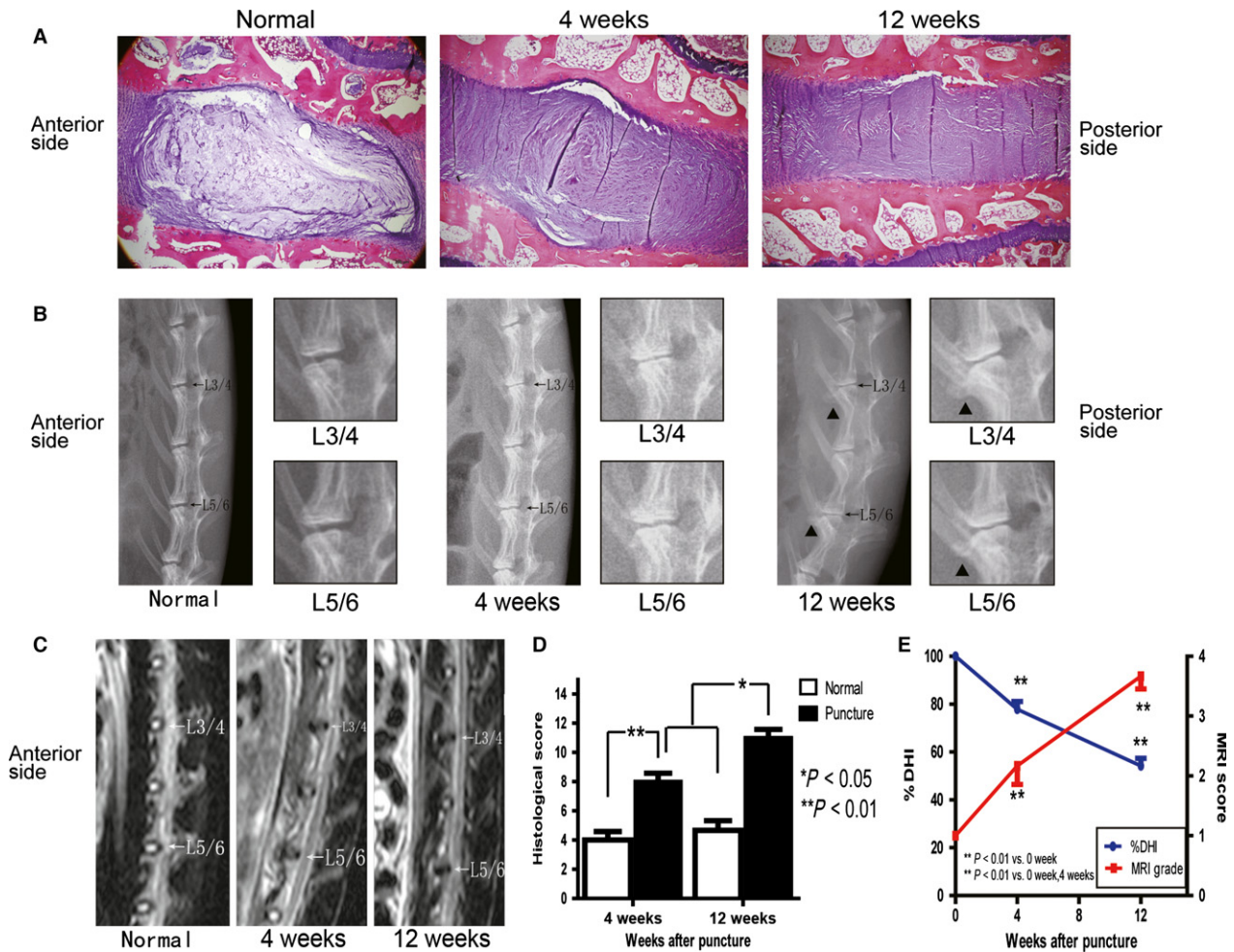


Fig. 1 Altered histological, radiographic and magnetic resonance imaging (MRI) results of the intervertebral discs (IVDs) after needle puncture. (A) Typical sections stained with hematoxylin and eosin (H & E; 40 ×) are shown. (B) Radiograph showing a decrease in the L3–4 and L5–6 disc height accompanied by endplate sclerosis and the formation of vertebral osteophytes (black triangle). The L3–4 and L5–6 discs are enlarged in the right panel. (C) Decreased signal intensity of the punctured discs upon MRI imaging. (D) Histological changes in IVDs after puncture were evaluated using a grading score, and all data are presented as the mean ± standard deviation (SD). * $P < 0.05$, ** $P < 0.01$, $n = 6$. (E) Decreased % disc height index (DHI) of the punctured discs and gradually increased MRI score using modified Thompson classification. All the data are presented as the mean ± SD. ** $P < 0.01$, $n = 6$ discs from three rabbits.

lumen for digestion and extrusion (Fig. 4C). The vacuoles were depleted, and only the nucleus remained. Finally, the cell contained only a hyper-condensed nucleus, accompanied by a few rER membranes, indicating that the cell was on the verge of death (Fig. 4D).

Late stage of chondroptosis. The late stages were characterized by the condensation of the nucleus and disintegration of ER membranes into vesicular detritus (Fig. 4E,F), which is represented by the dark particles surrounding the normal cell.

In brief, the process of chondroptosis entailed progressive extrusion, secretion and disintegration of the cell including the cytoplasm, organelles and nuclear remnants.

Despite extensive ultrastructural studies involving apoptosis in IVDs, classic apoptosis was rarely seen in the NP

(Fig. 3C). We found that the percentage of chondroptotic cells was significantly higher than that of apoptotic cells at 4 and 12 weeks after puncture in the same discs ($P = 0.025$, $P = 0.044$; Fig. 4G). Furthermore, compared with that observed in the normal discs, the punctured nucleus contained significantly more dark cells (at 4 weeks, $P = 0.021$; at 12 weeks, $P = 0.005$). However, the number of classical apoptotic cells in these groups was similar ($P > 0.05$), although it appeared that the apoptotic percentage was greater at 12 weeks than in control. Due to the inconspicuous differences separating the three stages of the cells, we failed to observe a precise distribution of these cells in different types of NP tissue. However, we found that the severely degenerated NP contained a higher number of dark cells in the mid- and late stages.

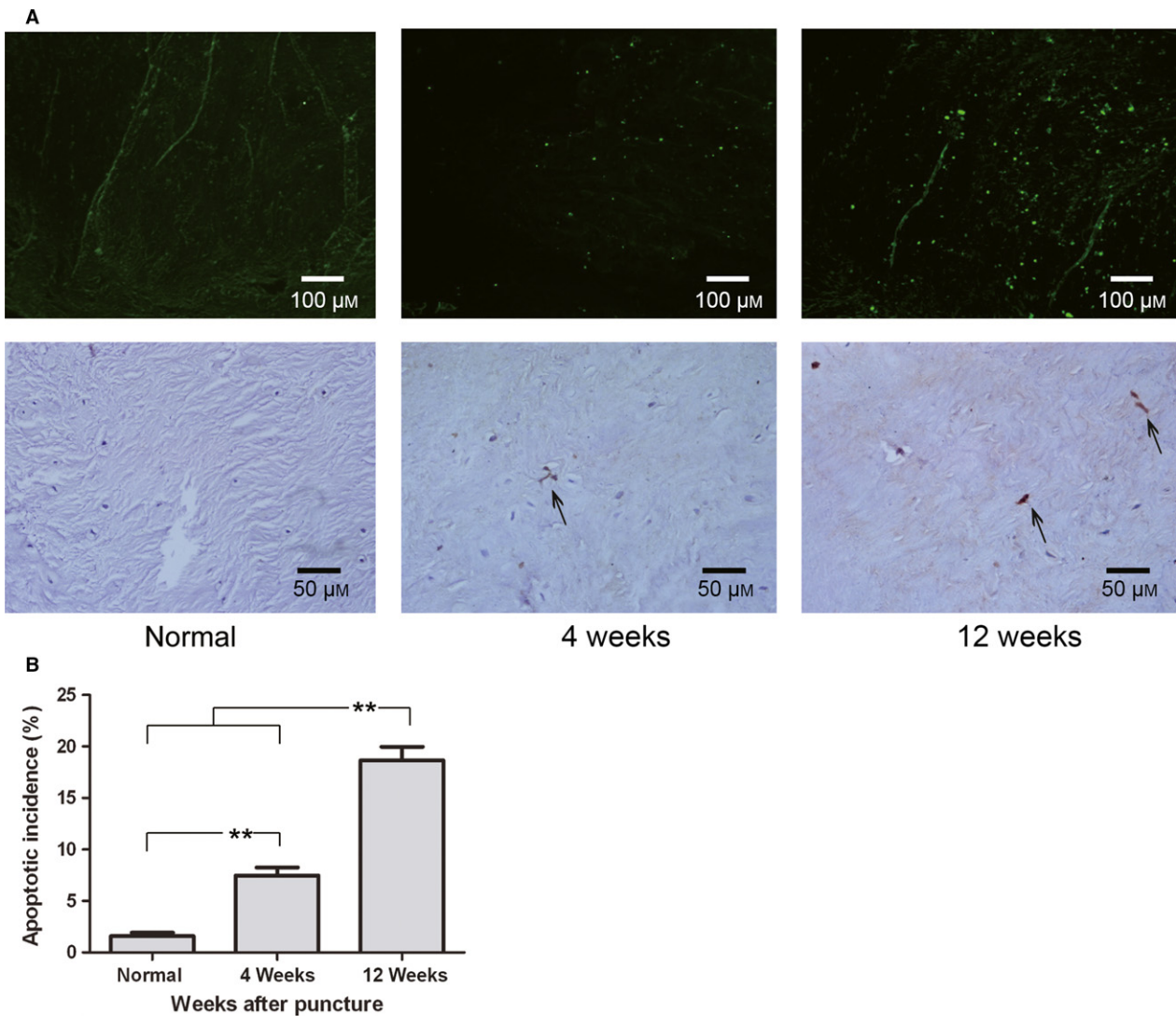


Fig. 2 Apoptosis in the nucleus pulposus (NP) detected by TUNEL staining. (A) Apoptotic cells were visualized using fluorescence microscopy and light microscopy (200 ×, 400 ×). (B) Quantification of the apoptotic incidence between groups. Apoptosis varied significantly at each time point after puncture. ** $P < 0.01$, values represent the mean \pm SD of six discs from three rabbits.

Because of the non-normal distribution of these variables, the Bland–Altman method was used to evaluate the reproducibility of counting the number of apoptotic and chondroptotic cells under TEM. As shown in Fig. S1, the mean differences of all parameters including the apoptotic and chondroptotic cell number were close to the '0' value. In addition, only one dot was located outside of the limits of agreements in Fig. S1B–D, indicating good reproducibility of the cell number counts.

Paralyzed cells

Dark cells were absent in the herniated tissue. However, a few strange cells, designated 'paralyzed' cells, presented with morphology that was different from that of the normal chondrocyte-like and dark cells. First, the cytoplasm of these cells was occupied by a considerable number of ER membranes, and the remaining cytoplasm was enclosed by

the expanded ER lumen. As described by Roach & Clarke (1999), the cytoplasm resembled an 'island' within a 'lake' of rER lumen (Fig. 5C). The cytoplasm and organelles were digested by an unknown mechanism. However, no nuclear condensation occurred as opposed to that observed in the dark cells. Finally, a few ER membranes showed dark, worm-like inclusions (Fig. 5E) together with a few Golgi complexes, vesicles and swollen mitochondria (Fig. 5F). The nucleus was condensed with convoluted morphology and patches of chromatin, representing a paralyzed state.

Expression of caspase 3 and 58K Golgi protein in the NP

Caspase 3 is the executioner of cell death. Therefore, we used Western blot to analyze caspase 3 expression in the punctured NP (Fig. 6A). Compared with the protein levels

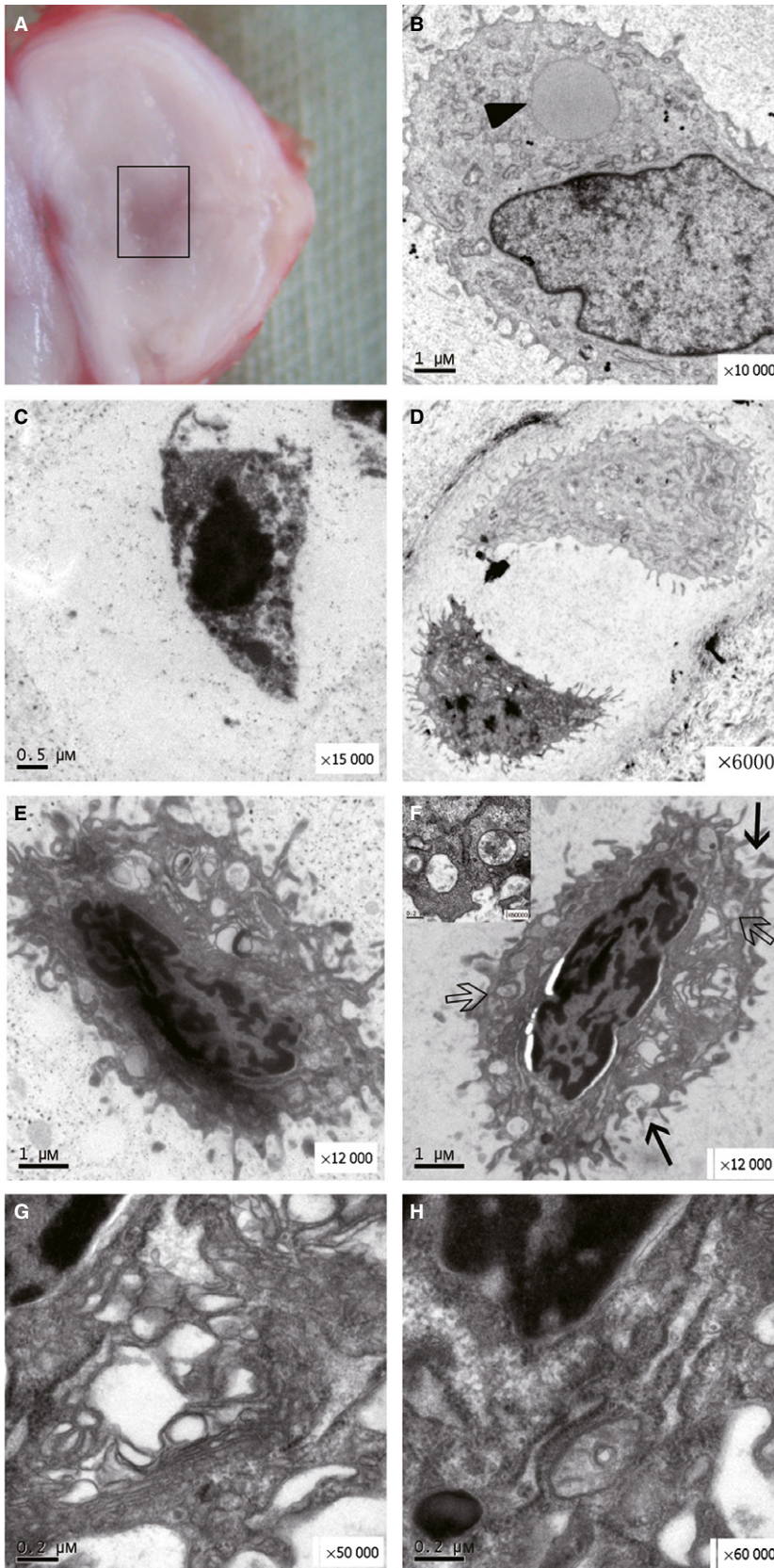


Fig. 3 Gross morphology of a punctured disc at 4 weeks along with various cells in the nucleus pulposus (NP). (A) The location and scope of the TEM sample are shown by the rectangle. (B) A healthy NP cell resembling a chondrocyte with a characteristic large lipid (black triangle) and a few endoplasmic reticulum (ER) membranes. (C) A classical apoptotic body with nuclear chromatin condensation into a crescent and a shrunken cell membrane. (D) Single dark cell in a doublet with a light cell in one lacuna. (E,F) Two typical chondroptotic cells in the early stage with many vacuoles (hollow arrow and inset) and a ruptured cell membrane (black arrows; $\times 12\,000$). (G,H) Two figures enlarged from (F) ($\times 50\,000$, $\times 60\,000$) showing abundant Golgi complexes and rER.

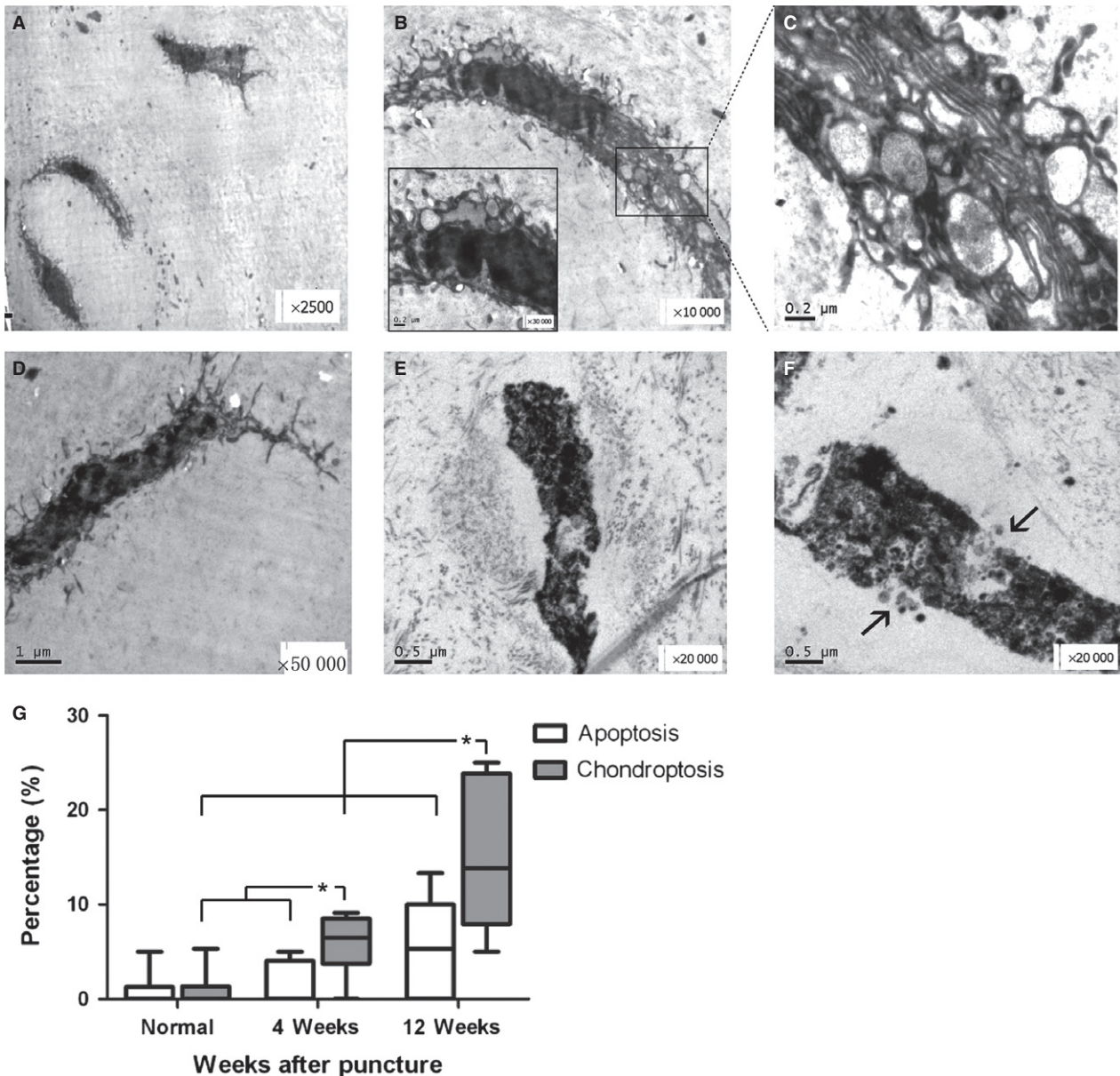


Fig. 4 Chondroptotic nucleus pulposus (NP) cells in the middle and late stages at 12 weeks, and the percentage of apoptotic and chondroptotic cells in all NP cells. (A) Three darker chondroptotic cells located in two lacunae surrounded by dark debris with long spindle morphology ($\times 2500$). (B) A typical mid-stage spindle-shaped chondroptotic cell with endoplasmic reticulum (ER) membranes and vacuoles ($\times 10\,000$). The area in the rectangle was enlarged in (C). (C) Extensive ER membranes enclosing segments of organelles and cytoplasm, with vacuoles discharged into the lacuna ($\times 50\,000$). (D) A chondroptotic cell with a few condensed ER membranes around the nucleus ($\times 12\,000$). (E, F) Two cell remnants in the late stage of chondroptosis showing disintegration and secretion of the debris into the extracellular space (black arrow, $\times 20\,000$). (G) Upper and lower extremes are shown by bars. The median (horizontal line) and 25% and 75% percentiles are shown by the box. $*P < 0.05$, $n = 12$ discs from six rabbits each group.

in normal and punctured NP tissue at 4 weeks, densitometry revealed a significant increase in caspase 3 levels at 12 weeks after puncture ($P < 0.01$; Fig. 6B). The 58K protein is the marker of the Golgi apparatus. Its relative expression increased significantly at 4 weeks after puncture compared with that of the normal group ($P = 0.019$; Fig. 6). At 12 weeks after NP puncture, the relative expression of the 58K

Golgi protein was decreased compared with the levels at 4 weeks ($P = 0.06$; Fig. 6).

Discussion

Chondroptotic cells were first observed in the early growth plate of rabbits' femurs (Erenpreisa & Roach, 1998; Roach &

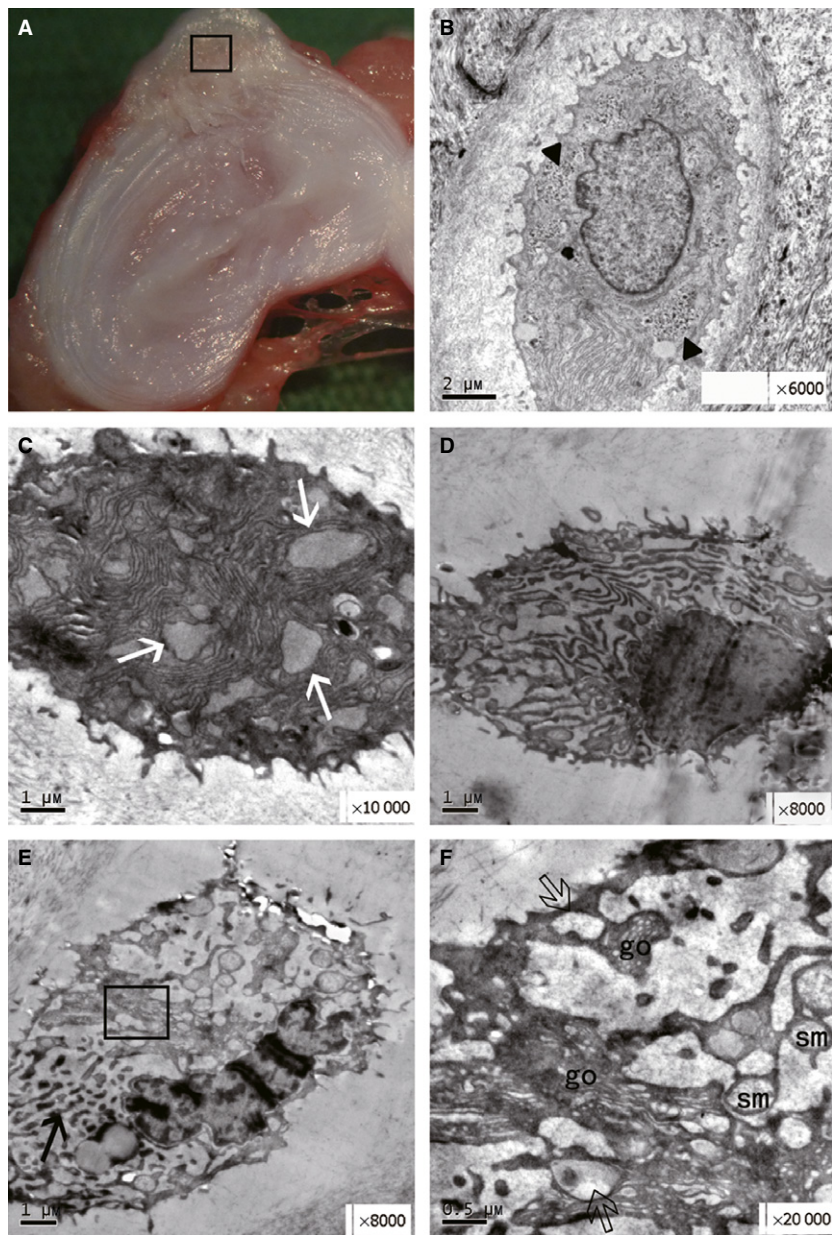
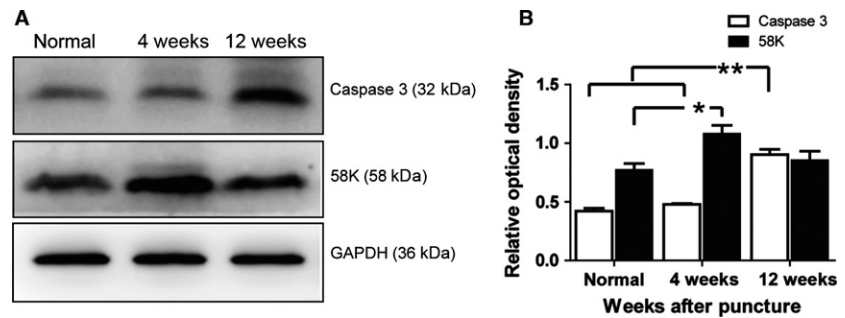


Fig. 5 Gross morphology of the punctured disc and cells in the herniated tissue at 12 weeks. (A) Location and scope of the EM sample obtained from the herniated tissue (square). (B) A normal cell with light cytoplasm and glycogen deposition (black triangle $\times 6000$). (C) Extensive endoplasmic reticulum (ER) membranes (white arrow $\times 10\,000$) in the cytoplasm of early-stage chondroptosis. (D) The cell had a normal nucleus with a partly digested cytoplasm ($\times 8000$). (E) Dark and worm-like inclusions in the cytoplasm, indicating the state of 'paralysis' (black arrow), and nuclear condensation with patchy chromatin. (F) Enlarged square showing vesicles (hollowed arrow), Golgi apparatus (go) and swollen mitochondria (sm) in the cytoplasm.

Clarke, 2000). Cartilage in the growth plate is an avascular structure, similar to the IVDs. Previous studies have described chondroptotic cells in the degenerated discs of patients (Sitte et al. 2009, 2012), while the ultrastructure morphology of classic apoptosis has not been reported in the herniated NP. In these studies, only the chondroptotic cells in the early stage were analyzed, ignoring cells in the middle and late stages. However, we found that the

ultrastructural morphology of chondroptosis was different across the different stages. Therefore, the present study was the first research to systematically study chondroptosis across all stages in a needle-puncture rabbit model of IDD. According to the classification described in a previous paper (Adams & Dolan, 2012), IDD could be classified into two types, including endplate-driven type A and annulus-driven type B. The disc degeneration in the present study might

Fig. 6 Expression of caspase 3 and the 58K protein in the nucleus pulposus (NP) at different times after puncture. (A) The images represent the caspase 3 and 58K Golgi protein of the NP at 4 and 12 weeks after puncture, respectively. (B) Quantitative analysis of caspase 3 and 58K protein levels illustrated by caspase 3/ β -actin and 58K/ β -actin. Values represent the mean \pm SD. * $P < 0.05$, ** $P < 0.01$, $n = 3$.



belong to the B degeneration due to the fissures in the AF induced by the puncture. The change in the NP cells in the present study might be a response to the sudden drop in the NP pressure. However, there is no definite evidence supporting this speculation.

Recently, several studies focusing on apoptosis in aged or degenerated IVDs of patients based on TEM have revealed condensed nuclear chromatin and shrunken cell membranes (Postacchini et al. 1984; Ahsan et al. 2001; Gruber & Hanley, 2002). The ultrastructural morphology of these cells met the criteria of chondroptosis, including a convoluted nucleus, patchy chromatin condensation, extensive blebbing, and abundant ER membranes and Golgi complexes. Gruber & Hanley, (2002) described the rupture of specific areas of the cellular membrane of apoptotic human disc cells in the early apoptotic stage. Our findings indicate that the membranes of the classic apoptotic cells were intact, and death with 'dignity' was used to prevent the leakage of excitatory amino acids, proteolytic enzymes, DNA and oxidized lipids in a proinflammatory response (Bacigalupo et al. 2007). Therefore, chondroptosis occurred as a variation of apoptosis that had already been observed, but the researchers failed to detect it.

By using the TUNEL method, the apoptotic incidence of the NP cells was significantly different across groups in this study. Interestingly, at 12 weeks, the total proportion of chondroptotic and apoptotic cells calculated under TEM was similar to the apoptotic incidence detected by the TUNEL assay (approximately 18%). Consistent with other studies (Grasl-Kraupp et al. 1995), we indirectly found that all of the apoptotic and chondroptotic cells showed DNA breakage using the TUNEL assay. If the TUNEL method was used to evaluate the incidence of classical apoptosis in the IVD cells of various models, the percentage of chondroptotic cells should be deducted to prevent an artificial exaggeration. However, most previous studies related to apoptosis in IVDs used the TUNEL assay to detect the incidence of apoptosis, and the majority of the 'apoptotic cells' probably showed chondroptosis.

The main characteristic of osteoarthritis and IDD is the loss of viable chondrocytes and NP cells (Blanco et al. 1998; Sharif et al. 2004; Zhao et al. 2006). However, the type of cell death remains controversial. Co-localization of the

Golgi complexes with caspase-2L in the TUNEL-positive cells and the presence of a higher number of Golgi complexes in the chondrocytes of human osteoarthritic cartilage than normal cartilage indicate that chondroptosis might be the predominant type of programmed cell death in cartilage (Perez et al. 2005; Zamli & Sharif, 2011). In the present study, the gradual degeneration of the punctured discs was demonstrated by using MRI and radiological and histological evaluation. Our study showed a significant increase in the number of dark cells in the severely degenerated NP compared with that in the moderate and normal specimens. In the discs at 12 weeks after puncture, a higher number of dark cells was observed in the middle and late stages. Furthermore, there were significantly more chondroptotic cells than apoptotic cells in the degenerated NP. Therefore, at least two important types of programmed cell death occurred in the disc, and chondroptosis may play a more important role in the development of NP degeneration. Chondroptosis should be further explored *in vivo* and *in vitro*. The culture system *in vitro*, including pellets, may also be used to induce chondroptosis of NP cells (Ahmed et al. 2007).

The 58K protein is a marker of the Golgi complex, and its expression was increased in the rabbit NP 4 weeks after the operation, but declined later in the present study. At the same time, chondroptotic cells in the early stage were filled with extensive Golgi complexes that were then digested and secreted into the extracellular space in the middle and late stages. Kouri et al. (2002) found that the Golgi labeling intensity was decreased in the rat osteoarthritic cartilage by day 45 after surgery; however, Perez et al. (2005) found that the intensity was increased in human osteoarthritic cartilage. The notion that the rat cartilage was completely destroyed in 60 days after surgery could explain the above discrepancy (Perez et al. 2005). Therefore, the severity of the degeneration might determine the number of Golgi in the cytoplasm. In our study, the NP changes and degeneration of the rabbit discs were slow and developed gradually, mimicking the alteration in the human discs by using the puncture model. Previous studies have proven that degeneration begins at 4 weeks after puncture in the rabbit IDD model (Masuda et al. 2005; Sobajima et al.

2005), accounting for the increase in 58K expression at 4 weeks after the operation.

Ahmed et al. (2007) found that staurosporine induced apoptosis of fetal horses chondrocytes cultured in a monolayer but chondroptosis of chondrocytes cultured in pellets similar to those seen *in vivo*. Apoptosis and chondroptosis might share similar pathways *in vivo*, resulting in the possible confusion reported in the previous studies related to apoptosis in IVDs. The ER pathway has been demonstrated in the degenerative rat IVDs and the cultured rat AF cells, and *in vivo* silencing of CHOP (C/EBP homologous protein) even attenuated disc degeneration (Zhao et al. 2010; Zhang et al. 2011). The abundant rER membranes in the cytoplasm observed in the present study suggested that the ER pathway also played an important role in chondroptosis. Additionally, in other degenerative diseases, activation of caspase 3, known as a death executioner and the main apoptosis executor, was also induced by the activation of the ER stress pathway (Song et al. 2002; Hitomi et al. 2004). Although the expression of caspase 3 was increased in the degenerative discs, the precise role of caspase 3 in chondroptosis needs to be explored in the future.

The ultimate fate of the dark cells is controversial, although some studies have reported that healthy chondrocytes occasionally engulf the dark cells and apoptotic bodies in embryonic chick femurs and in chondrocyte pellet cultures (Erenpreisa & Roach, 1996, 1998; Ahmed et al. 2007). The bovine NP cell may potentially act as a phagocyte *in vitro* (Jones et al. 2008), but we did not observe a similar phenomenon. Instead, the remnants in the lacunae gradually disintegrated into debris, leaving the empty nests, and the debris were absorbed and became a part of the extracellular matrix (Burdan et al. 2009). The debris of dead human NP cells constitute the encircling layers of the extracellular matrix surrounding the healthy cells (Gruber & Hanley, 2002), which may be absorbed during degeneration or tissue calcification (Loreto et al. 2011).

Dark cells were found in the NP, whereas paralyzed cells were present in the herniated tissue containing the osteophytes, indicating a role of the environment in the development of specific cell death types in IVDs. The definition of 'paralyzed' cells came from a previous paper (Roach & Clarke, 2000). The word 'paralyzed' means that these cells appear to be 'in limbo', where the lumen of the ER fills the entire cytoplasm with dark and worm-like inclusions, resulting in a fewer number of organelles (Roach & Clarke, 2000). The extensive rER membranes of the paralyzed cells suggested that they are a subtype of dark cell. The present study is the first report of 'paralyzed' cells in a needle-punctured model of IDD.

A major limitation of this study is that the needle-puncture-induced IDD does not absolutely reflect the process of degeneration in human discs, although an ideal model still needs to be identified.

In summary, chondroptosis is distinguished from apoptosis based on the ultrastructural morphology. *In vivo*, this study demonstrated that chondroptosis is a major type of programmed cell death in IVDs and elucidated its relationship with IDD. Previous studies investigating apoptosis should be reviewed to further elucidate the role of chondroptosis in IDD.

Acknowledgements

This work is supported by the Natural Science Foundation of China (81501869, 81601980).

Author contributions

En-Xing Xue conceived the experiments. Li-Bo Jiang designed and performed all of the experiments. Hai-Xiao Liu designed and conducted the Western blotting analyses. Yu-Long Zhou and Sun-Ren Sheng analyzed the results. All authors reviewed the manuscript.

Conflict of interest

The authors declare that they have no conflict of interest.

References

- Adams MA, Dolan P (2012) Intervertebral disc degeneration: evidence for two distinct phenotypes. *J Anat* **221**, 497–506.
- Ahmed YA, Tatarczuch L, Pagel CN, et al. (2007) Physiological death of hypertrophic chondrocytes. *Osteoarthritis Cartilage* **15**, 575–586.
- Ahsan R, Tajima N, Chosa E, et al. (2001) Biochemical and morphological changes in herniated human intervertebral disc. *J Orthop Sci* **6**, 510–518.
- Anderson DR (1964) The ultrastructure of elastic and hyaline cartilage of the rat. *Am J Anat* **114**, 403–434.
- Bacigalupo F, Huerta D, Montefusco-Siegmund R (2007) The debate about death: an imperishable discussion? *Biol Res* **40**, 523–534.
- Blanco FJ, Guitian R, Vazquez-Martul E, et al. (1998) Osteoarthritic chondrocytes die by apoptosis. A possible pathway for osteoarthritic pathology. *Arthritis Rheum* **41**, 284–289.
- Burdan F, Szumilo J, Korobowicz A, et al. (2009) Morphology and physiology of the epiphyseal growth plate. *Folia Histochem Cytobiol* **47**, 5–16.
- Chen KS, Tatarczuch L, Ahmed Y, et al. (2010) Identification of light and dark hypertrophic chondrocytes in mouse and rat chondrocyte pellet cultures. *Tissue Cell* **42**, 121–128.
- Ding F, Shao ZW, Yang SH, et al. (2012) Role of mitochondrial pathway in compression-induced apoptosis of nucleus pulposus cells. *Apoptosis* **17**, 579–590.
- Erenpreisa J, Roach HI (1996) Epigenetic selection as a possible component of transdifferentiation. Further study of the commitment of hypertrophic chondrocytes to become osteocytes. *Mech Ageing Dev* **87**, 165–182.
- Erenpreisa J, Roach HI (1998) Aberrant death in dark chondrocytes of the avian growth plate. *Cell Death Differ* **5**, 60–66.

- Grasl-Kraupp B, Ruttkay-Nedecky B, Koudelka H, et al. (1995) In situ detection of fragmented DNA (TUNEL assay) fails to discriminate among apoptosis, necrosis, and autolytic cell death: a cautionary note. *Hepatology* **21**, 1465–1468.
- Gruber HE, Hanley EN Jr (2002) Ultrastructure of the human intervertebral disc during aging and degeneration: comparison of surgical and control specimens. *Spine (Phila Pa 1976)* **27**, 798–805.
- Gruber HE, Norton HJ, Hanley EN Jr (2000) Anti-apoptotic effects of IGF-1 and PDGF on human intervertebral disc cells in vitro. *Spine (Phila Pa 1976)* **25**, 2153–2157.
- Hitomi J, Katayama T, Taniguchi M, et al. (2004) Apoptosis induced by endoplasmic reticulum stress depends on activation of caspase-3 via caspase-12. *Neurosci Lett* **357**, 127–130.
- Jones P, Gardner L, Menage J, et al. (2008) Intervertebral disc cells as competent phagocytes in vitro: implications for cell death in disc degeneration. *Arthritis Res Ther* **10**, R86.
- Kakisaka K, Cazanave SC, Fingas CD, et al. (2012) Mechanisms of lysophosphatidylcholine-induced hepatocyte lipoapoptosis. *Am J Physiol Gastrointest Liver Physiol* **302**, G77–G84.
- Kelempisioti A, Eskola PJ, Okuloff A, et al. (2011) Genetic susceptibility of intervertebral disc degeneration among young Finnish adults. *BMC Med Genet* **12**, 153.
- Kerr JF, Wyllie AH, Currie AR (1972) Apoptosis: a basic biological phenomenon with wide-ranging implications in tissue kinetics. *Br J Cancer* **26**, 239–257.
- Kouri JB, Rojas L, Perez E, et al. (2002) Modifications of Golgi complex in chondrocytes from osteoarthrotic (OA) rat cartilage. *J Histochem Cytochem* **50**, 1333–1340.
- Loreto C, Musumeci G, Castorina A, et al. (2011) Degenerative disc disease of herniated intervertebral discs is associated with extracellular matrix remodeling, vimentin-positive cells and cell death. *Ann Anat* **193**, 156–162.
- Masuda K, Aota Y, Muehleman C, et al. (2005) A novel rabbit model of mild, reproducible disc degeneration by an annulus needle puncture: correlation between the degree of disc injury and radiological and histological appearances of disc degeneration. *Spine (Phila Pa 1976)* **30**, 5–14.
- Millucci L, Giorgetti G, Viti C, et al. (2015) Chondroptosis in alkaptanuric cartilage. *J Cell Physiol* **230**, 1148–1157.
- Miyagi M, Millecamps M, Danco AT, et al. (2014) ISSLS Prize winner: increased innervation and sensory nervous system plasticity in a mouse model of low back pain due to intervertebral disc degeneration. *Spine (Phila Pa 1976)* **39**, 1345–1354.
- Paul CP, Zuiderbaan HA, Zandieh Doulabi B, et al. (2012) Simulated-physiological loading conditions preserve biological and mechanical properties of caprine lumbar intervertebral discs in ex vivo culture. *PLoS One* **7**, e33147.
- Perez HE, Luna MJ, Rojas ML, et al. (2005) Chondroptosis: an immunohistochemical study of apoptosis and Golgi complex in chondrocytes from human osteoarthrotic cartilage. *Apoptosis* **10**, 1105–1110.
- Postacchini F, Bellocchi M, Massobrio M (1984) Morphologic changes in annulus fibrosus during aging. An ultrastructural study in rats. *Spine (Phila Pa 1976)* **9**, 596–603.
- Roach HI, Clarke NM (1999) "Cell paralysis" as an intermediate stage in the programmed cell death of epiphyseal chondrocytes during development. *J Bone Miner Res* **14**, 1367–1378.
- Roach HI, Clarke NM (2000) Physiological cell death of chondrocytes in vivo is not confined to apoptosis. New observations on the mammalian growth plate. *J Bone Joint Surg Br* **82**, 601–613.
- Roach HI, Aigner T, Kouri JB (2004) Chondroptosis: a variant of apoptotic cell death in chondrocytes? *Apoptosis* **9**, 265–277.
- Roberts S, Evans H, Trivedi J, et al. (2006) Histology and pathology of the human intervertebral disc. *J Bone Joint Surg Am* **88** (Suppl 2), 10–14.
- Samartzis D, Karppinen J, Chan D, et al. (2012) The association of lumbar intervertebral disc degeneration on MRI in overweight and obese adults: a population-based study. *Arthritis Rheum* **64**, 1488–1496.
- Sharif M, Whitehouse A, Sharman P, et al. (2004) Increased apoptosis in human osteoarthrotic cartilage corresponds to reduced cell density and expression of caspase-3. *Arthritis Rheum* **50**, 507–515.
- Sitte I, Kathrein A, Pfaller K, et al. (2009) Intervertebral disc cell death in the porcine and human injured cervical spine after trauma: a histological and ultrastructural study. *Spine (Phila Pa 1976)* **34**, 131–140.
- Sitte I, Kathrein A, Pedross F, et al. (2012) Morphological changes in disc herniation in the lower cervical spine: an ultrastructural study. *Eur Spine J* **21**, 1396–1409.
- Sobajima S, Kompel JF, Kim JS, et al. (2005) A slowly progressive and reproducible animal model of intervertebral disc degeneration characterized by MRI, X-ray, and histology. *Spine (Phila Pa 1976)* **30**, 15–24.
- Song L, De Sarno P, Jope RS (2002) Central role of glycogen synthase kinase-3beta in endoplasmic reticulum stress-induced caspase-3 activation. *J Biol Chem* **277**, 44 701–44 708.
- Sudo H, Minami A (2011) Caspase 3 as a therapeutic target for regulation of intervertebral disc degeneration in rabbits. *Arthritis Rheum* **63**, 1648–1657.
- Vo N, Wang D, Sowa G, et al. (2011) Differential effects of nicotine and tobacco smoke condensate on human annulus fibrosus cell metabolism. *J Orthop Res* **29**, 1585–1591.
- Wang WB, Feng LX, Yue QX, et al. (2012) Paraptosis accompanied by autophagy and apoptosis was induced by celastrol, a natural compound with influence on proteasome, ER stress and Hsp90. *J Cell Physiol* **227**, 2196–2206.
- Zamli Z, Sharif M (2011) Chondrocyte apoptosis: a cause or consequence of osteoarthritis? *Int J Rheum Dis* **14**, 159–166.
- Zhang YH, Zhao CQ, Jiang LS, et al. (2011) Cyclic stretch-induced apoptosis in rat annulus fibrosus cells is mediated in part by endoplasmic reticulum stress through nitric oxide production. *Eur Spine J* **20**, 1233–1243.
- Zhao CQ, Jiang LS, Dai LY (2006) Programmed cell death in intervertebral disc degeneration. *Apoptosis* **11**, 2079–2088.
- Zhao CQ, Wang LM, Jiang LS, et al. (2007) The cell biology of intervertebral disc aging and degeneration. *Ageing Res Rev* **6**, 247–261.
- Zhao CQ, Zhang YH, Jiang SD, et al. (2010) Both endoplasmic reticulum and mitochondria are involved in disc cell apoptosis and intervertebral disc degeneration in rats. *Age (Dordr)* **32**, 161–177.

Supporting Information

Additional Supporting Information may be found in the online version of this article:

Fig. S1. The Bland–Altman analysis for the consistency of the intra-observer and inter-observer evaluation.